Optimization of the process parameters for the removal of phosphate from drinking water by electrocoagulation

Subramanyan Vasudevan*, Jothinathan Lakshmi, Ganapathy Sozhan

Central Electrochemical Research Institute (CSIR), Karaikudi 630 006, India
Tel. +91 4565 227554; Fax +91 4565 227779; email: vasudevan65@gmail.com

ABSTRACT

The present studies provide the purification of drinking water containing phosphate by electrocoagulation process using zinc as the anode and stainless steel as the cathode. The experimental parameters like electrolyte pH, temperature and current density, and so forth, on the removal efficiency of phosphate were carried out. The adsorption capacity was evaluated using both Langmuir and Freundlich isotherm models. The kinetic studies show that the adsorption obeys second-order kinetics. The maximum removal efficiency of 98.8% was achieved at a current density of 0.05 A/dm^2, at a pH of 7.0. Thermodynamic parameters were evaluated. Overall adsorption process was endothermic and spontaneous. The adsorption of phosphate preferably fitting the Langmuir adsorption isotherm suggests monolayer coverage of adsorbed molecules.

Keywords: Electrocoagulation; Phosphate; Removal; Adsorption; Kinetics; Isotherms

1. Introduction

Eutrophication is one of the main problems nowadays encountered in the monitoring of environmental water sources in industrialized countries. This phenomenon, which is responsible for the dramatic growth of algae occurring in drinking water, is caused by the excess phosphate concentration in the effluents from municipal or industrial plants discharged to the environment. In the countryside, agriculture and animal husbandries are the main industries; wastes from these industries will contribute to the accumulation of phosphorus in soil and water bodies. These phosphorus compounds, dissolved in surface or groundwater, are responsible for eutrophication in closed water systems, especially in lakes and enclosed bays where the water is almost stagnant [1].

The US discharge limit of phosphate is 0.5–1.0 mg-P/L. The Indian discharge limits for phosphate is 5 mg-P/L [2].

To meet water quality standards, further treatment of water is required. Phosphate removal from wastewater has received considerable attention since the late 1960s [3]. Phosphate removal techniques fall into three main categories: physical, chemical, and biological. Physical methods have proven to be either too expensive, as in the case of electrodialysis or reverse osmosis, inefficient, removing only 10% of the total phosphate [4]. Chemical treatment is widely used for phosphate removal. The common chemicals used for treatments are aluminum sulfate and ferric chloride. At present, chemical treatments are not used due to disadvantages like high costs of maintenance, problems of sludge handling and its disposal, and neutralization of the effluent [5–7]. In a biological treatment plant, it is necessary to transfer phosphate from the liquid to the sludge phase, and the

* Corresponding author.

removal efficiency usually does not exceed 30%, which means that remaining phosphate should be removed by another technique [8]. The phosphate removal from wastewater by adsorption using different materials has also been explored. The major disadvantages of this studied adsorbent are low efficiency and high cost [9–15].

Recent research has demonstrated that electrochemistry offers an attractive alternative to above-mentioned traditional methods for treating wastewaters [16–22]. Electrochemical coagulation, which is one of these techniques, is the electrochemical production of destabilization agents that brings about charge neutralization for pollutant removal and it has been used for water or wastewater treatment. Usually, aluminum or iron plates are used as electrodes in the electrocoagulation process. Electrochemically generated metallic ions from these electrodes can undergo hydrolysis near the anode to produce a series of activated intermediates that are able to destabilize the finely dispersed particles present in the water/wastewater to be treated. The destabilized particles then aggregate to form flocs [23].

(i) When zinc is used as anode, the reactions are as follows:

At the cathode:

$$2H_2O + 2e^- \rightarrow H_2(g) + 2OH^- \tag{1}$$

At the anode:

$$Zn \rightarrow Zn^{2+} + 2e^- \tag{2}$$

In the solution:

$$Zn^{2+}(aq) + 2H_2O(l) \rightarrow Zn(OH)_2 + 2H^+ (aq) \tag{3}$$
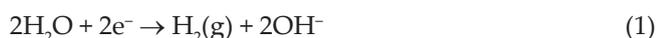
(ii) When aluminium is used as electrode, the reactions are as follows:

At the cathode:

$$2H_2O + 2e^- \rightarrow H_2 (g) + 2OH^- \tag{4}$$

At the anode:

$$Al \rightarrow Al^{3+} + 3e^- \tag{5}$$

In the solution:

$$Al^{3+}(aq) + 3H_2O \rightarrow Al(OH)_3 + 3H^+(aq) \tag{6}$$
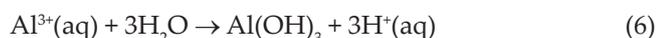
The advantages of electrocoagulation include high particulate removal efficiency, a compact treatment facility, relatively low cost, and the possibility of complete automation [24,25]. This method is characterized by reduced sludge production, a minimum requirement of chemicals and ease of operation [26]. Although there are numerous reports related with electrochemical coagulation as a means of removal of many pollutants from water and wastewater, there is limited work on phosphate removal by the electrochemical method and its adsorption and kinetics studies. This article presents the results of the laboratory scale studies on the removal of phosphate using zinc and stainless steel as the anode and cathode

respectively by the electrocoagulation process. In doing so, the equilibrium adsorption behavior is analyzed by fitting models of Langmuir and Freundlich isotherms. Adsorption kinetics of electrocoagulants is analyzed using first- and second-order kinetic models. Activation energy is evaluated to study the nature of adsorption.

2. Materials and methods

2.1. Cell construction and electrolysis

The electrolytic cell consisted of a 1.0-L Plexiglas vessel that was fitted with a poly-(vinyl chloride) (PVC) cell cover with slots to introduce the electrodes, pH sensor, a thermometer and the electrolytes. Zinc (commercial grade, India) with a surface area of 0.02 m² acted as the anode. The cathode was a stainless steel (SS 304; SAIL, India) sheet of the same size as that of anode and placed at an interelectrode distance of 0.005 m. The temperature of the electrolyte was controlled to the desired value with a variation of ±2 K by adjusting the rate of flow of thermostatically controlled water through an external glass-cooling spiral. A regulated direct current was supplied from a rectifier (10 A, 0–25 V; Aplab model).

The phosphate (KH_2PO_4) (Analar Reagent) was dissolved in tap (drinking) water for the required concentration. A 0.90 L portion of solution was used for each experiment, which was used as the electrolyte. The pH of the electrolyte was adjusted, if required, with 1 M HCl and 1 M NaOH solutions before adsorption experiments.

2.2. Analysis

The analysis of phosphate was carried out using the yellow vanodomolybdophosphoric acid method by a double beam spectrophotometer according to the Standard Methods for Examination of Water and Wastewater [27].

The surface morphology of the anode before and after treatment was analyzed by metallurgical microscope of type ZEISS, Germany. The SEM of zinc hydroxide was analyzed with a scanning electron microscope (SEM) made by Hitachi (model s-3000h). Electrocoagulatioan-by products were analyzed by a JEOL X-ray diffractometer (Type JEOL, Japan).

3. Results and discussion

3.1. Effect of initial phosphate concentration

The adsorption of phosphate is increased with an increase in phosphate concentration and remains constant after the equilibrium time. The adsorption of phosphate is calculated and the results are illustrated in Fig. 1. The equilibrium time was 20 min for all of the concentrations studied (10–40 mg-P/L). The amount of phosphate adsorbed (q_e) increased from 40.40 to 154.30 mg/g of $Zn(OH)_2$ as the concentration was increased from 10 to
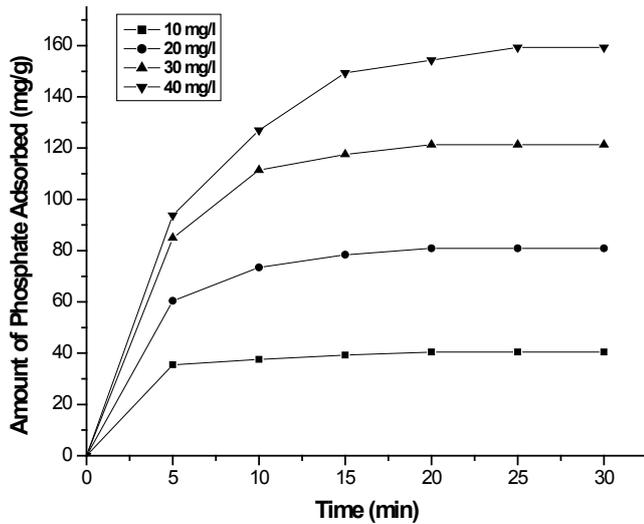
Fig. 1. Effect of agitation time and initial phosphate concentration on the amount of phosphate adsorbed. Electrolyte pH = 7.0, electrolyte temperature = 305 K and current density is 0.05 A.dm^{-2}

Fig. 2. Effect of pH on the removal of phosphate. Concentration of phosphate is 20 mg-P.L^{-1}, current density is 0.05 A.dm^{-2}, agitation time is 60 min and electrolyte temperature is 305 K.

40 mg-P/L. The figure also shows that the adsorption is rapid in the initial stages and gradually decreases with the progress of adsorption. The plots are single, smooth and continuous curves leading to saturation, suggesting the possible monolayer coverage to phosphate on the surface of the adsorbent [28].

3.2. Effect of pH

The electrolyte pH is one of the important factors affecting the performance of the electrochemical process. To examine this effect, a series of experiments were carried out using (20 mg-P.L^{-1}) phosphate-containing water, with an initial pH varying in the range of 2–12. The removal efficiency of phosphate was increased with increasing the pH and the maximum removal efficiency was obtained at pH 7 is shown in Fig. 2. According to Zn-H$_2$O Pourbaix diagram [29] and in thermodynamic point of view, that the precipitation of Zn(OH)$_2$ would only be significant at pH ≥ 8.6, however, the interfacial pH-increase during the electrocoagulation process favored the zinc hydroxide formation and resulting higher removal efficiency at pH 7.0. From the figure it is found that, the minimum removal efficiency obtained was 50% at pH 12. This is because, at alkaline pH the oxide surface has a net negative charges and would tend to repulse the anionic phosphate in solution. Therefore, the maximum amount of phosphate removal occurred at pH 7.

3.3. Effect of current density

The amount of phosphate removal and the removal rate have increased by increasing the current density.

The removal efficiencies are 35, 78, 88.86, 93 and 98.8% for current densities of 0.01, 0.02, 0.03, 0.04 and 0.05 A/dm^2 respectively. The results are presented in Fig. 3. From the figure it is found that, beyond 0.05 A/dm^2 the increase in removal efficiency is marginal and the voltage is very high at higher current densities. Hence, further studies were carried out only at 0.05 A/dm^2 . Further, the amount of phosphate removal depends upon the quantity of adsorbent generated, which is related to the time and current density [30,31]. The amount of adsorbent (Zn (OH)$_2$) was determined from the Faraday law [32].

$$E_c = ItM / ZF \qquad (7)$$

where I is current (A), t is the time (s), M is the molecular weight (M = 65.39 g/mol), Z is the electron involved, and F is the Faraday constant (96485.3 coulomb/mole). As expected, the amount of phosphate adsorption increases with the increase in current density, which indicates that the adsorption depends upon the availability of binding sites for phosphate (Fig. 3).

3.4. Adsorption kinetics

The adsorption kinetic data of phosphate are analyzed using the Lagergren rate equation. The first-order Lagergren model [33] and the rate expression is given by:

$$dq_t / dt = k_1 \left(q_e - q_t \right) \qquad (8)$$

where q_t is the amount of phosphate adsorbed on the adsorbent at time t (min) and k_1 (1/min) is the rate constant
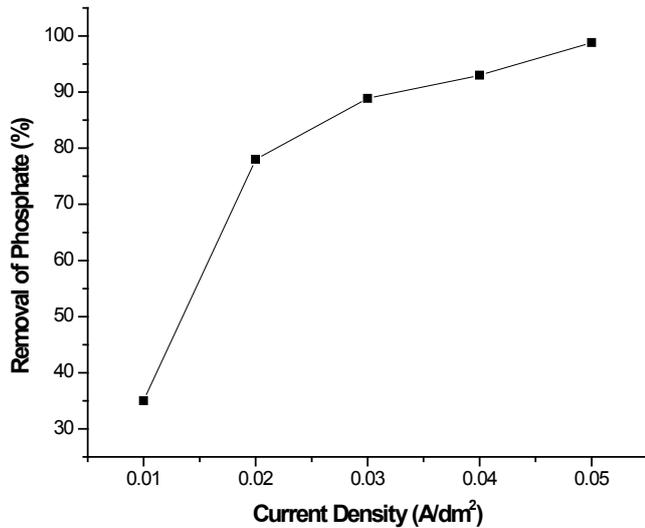
Fig. 3. Effect of current density on the removal of phosphate. Concentration of phosphate is 20 mg-P.L^{-1}, electrolyte pH is 7.0, agitation time is 60 min and electrolyte temperature is 305 K.

Fig. 4. Second-order kinetic model plot of different concentrations of phosphate. Electrolyte pH is 7.0, electrolyte temperature is 305 K and current density is 0.05 A.dm^{-2}.

of first order adsorption. The integrated form of the above equation with the boundary conditions ($t = 0$ to $t = t$ and $q_t = 0$ to $q_t = q_t$) can be written as

$$\log\left(q_e - q_t\right) = \log q_e - k_1 t / 2.303 \tag{9}$$

where q_e is the amount of phosphate adsorbed at equilibrium. The q_e and rate constant (k_1) were calculated from the slope of the plots of $\log\left(q_e - q_t\right)$ vs. time (t). A straight line obtained from the plots suggests the applicability of this kinetic model. It was found that the calculated q_e values do not agree with the experimental values (figure not shown here). So, the adsorption does not obey the first-order kinetics model.

The second-order kinetic model is expressed as [34]

$$dq_t / dt = k_2\left(q_e - q_t\right)^2 \tag{10}$$

where k_2 is the rate constant of the second-order adsorption. The integrated form of Eq. (10) with the boundary conditions ($t = 0$ to $t = t$ and $q_t = 0$ to $q_t = q_t$) can be written as

$$1/\left(q_e - q_t\right) = 1/q_e + k_2 t \tag{11}$$

Eq. (11) can be rearranged and linearized as

$$t / q_t = 1 / k_2 q_e^2 + t / q_e \tag{12}$$

The plot t/q_t vs. time (t) shows a straight line (Fig. 4). The second-order kinetic values of q_e (mg/g) and k_2 (g/mg min) were calculated from the slope and intercept of the plots t/q_t vs. t. The larger the k_2 value, the slower the adsorption rate, and the lower value of the k_2 indicates the faster the adsorption rate. The plot shows that the correlation coefficient for the second-order kinetic model obtained in all of the concentrations studied were above 0.99, and also the calculated q_e values agree with the experimental q_e values. Table 1 depicts the computed result obtained from the second-order kinetic model. These results indicate that the adsorption system studied belongs to the second-order kinetic model. Similar phenomena have been observed in the adsorption of phosphate in Fe(III)/Cr(III) hydroxide [28].

Table 1
Comparison between the experimental and calculated q_e values for different initial phosphate concentrations in second order adsorption isotherm at temperature 305 K and pH 7

Initial concentration of phosphate (mg-P.L^{-1})	q_e experimental (mg/g)	k_2 (g/mg-min)	q_e calculated (mg/g)	R^2
10	40.40	0.0218	40.12	0.9998
20	80.86	0.0092	79.84	0.9990
30	121.30	0.0036	120.16	0.9990
40	154.30	0.0011	189.39	0.9990

3.5. Adsorption isotherm

The adsorption capacity of the adsorbent has been tested using Freundlich [31] and Langmuir [28] isotherms. To determine the isotherms, the initial pH was kept at 7.0 and the concentration of phosphate used was in the range of 10–40 mg-P.L^{-1}. The general form of Freundlich adsorption isotherm is represented by [35]

$$q_e = KC^n \qquad (13)$$

Eq. (13) can be linearized in logarithmic form, and the Freundlich constants can be determined as follows [36]

$$\log q_e = \log k_f + n \log C_e \qquad (14)$$

where k_f is the Freundlich constant related to adsorption capacity, n is the energy or intensity of adsorption, and C_e is the equilibrium concentration of the phosphate (mg-P.L^{-1}). To determine the isotherms, the phosphate concentration used was 10–40 mg-P.L^{-1} at initial pH 7. The Freundlich constants k_f and n values were determined by the plot of log C_e vs. log q_e. The Freundlich constants k_f and n values are 4.3320 mg/g and 0.9730 L/mg respectively. It has been reported that values of n lying between 0 and 10 indicate favorable adsorption. From the analysis of the results it is found that the Freundlich plots do not fit satisfactorily with the experimental data obtained in the present study. This agrees well with the results presented in the literature [28].

Hence, the Langmuir isotherm has been used to study the surface monolayer adsorption with uniform energies of adsorption on the surface and no transmigration of adsorbate in the plane of the surface. The Langmuir isotherm is expressed as [37]

$$C_e / q_e = 1/q_0 b + C_e / q_0 \qquad (15)$$

where C_e is the concentration of the phosphate solution (mg-P.L^{-1}) at equilibrium, q_o is the adsorption capacity (Langmuir constant) and b is the energy of adsorption. Fig. 5 shows the Langmuir plot with experimental data. The Langmuir plot is a better fit with the experimental data compare to Freundlich plots. The value of the adsorption capacity q_o was found to be 4.362 g.g^{-1}, which is higher than that of other adsorbents studied [28]. The lower value of the adsorption capacity of the adsorbent studied is due to the pH of the solution, which was found to be >8. 0. This condition is not favorable for the adsorption of phosphate (Fig. 2).

The essential characteristics of the Langmuir isotherm can be expressed as the dimensionless constant R_L [38]

$$R_L = 1/(1+bc_0) \qquad (16)$$

where R_L is the equilibrium constant, which indicates the type of adsorption b, and c_o is the Langmuir constant. The R_L values indicate the type of isotherm: irreversible ($R_L = 0$), favorable ($0 < R_L < 1$), linear ($R_L = 1$) or unfavorable
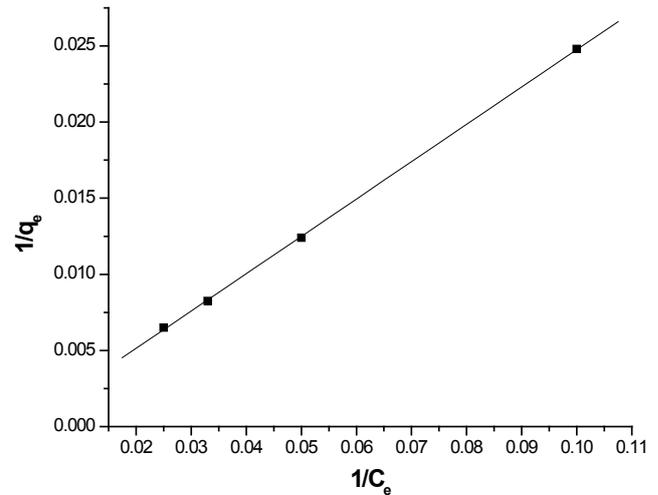
Fig. 5. Langmuir plot ($1/q_e$ vs. $1/C_e$). Electrolyte pH is 7.0, electrolyte temperature is 305 K and current density 0.05 A.dm^{-2}.

Table 2
Langmuir constants for the adsorption of phosphate at temperature 305 K and pH 7

Concentration of phosphate (mg-P.L^{-1})	q_0 (g/g)	b (l/g)	R_L
10	4.362	0.935	0.9907
20	4.362	0.935	0.9816
30	4.362	0.935	0.9727
40	4.362	0.935	0.9639

($R_L > 1$) [39]. In present study, the R_L values were found to be between 0 and 1 indicates that the adsorption is favourable. The results are presented in Table 2.

3.6. Effect of temperature

The amount of phosphate adsorbed on the adsorbent increases by increasing the temperature, indicating the process to be endothermic [40]. The diffusion coefficient (D) for the intraparticle transport of a PO$_4^{3-}$ species into the adsorbent particles has been calculated at different temperature by

$$t_{1/2} = 0.03 \times r_o^2 / D \qquad (17)$$

where $t_{1/2}$ is the time of half adsorption (s), r_o is the radius of the adsorbent particle (cm), and D is the diffusion coefficient (cm^2/s). For all chemisorption system the diffusivity coefficient should be 10^{-5}–10^{-13} cm^2/s [41]. In the present work, D is found to be in the range of 10^{-6} cm^2/s. The pore diffusion coefficient (D) values for different initial concentrations of PO$_4^{3-}$ and temperature are presented in Table 3.

Table 3
Pore diffusion coefficients for the adsorption of phosphate at temperature 305 K and pH 7

Initial phosphate concentration (mg-P.L^{-1})	Pore diffusion coefficient $D \times 10^6$ (cm^2/s)
10	0.9608
20	0.9272
30	0.8153
40	0.6353
Temperature (K)	
305	0.9272
313	0.7591
323	0.8090
333	0.8430

To find out the energy of activation for the adsorption of phosphate, the second-order rate constant is expressed in the Arrhenius form [42],

$$\log k_2 = \log k_0 - E / 2.303\, RT \tag{18}$$

where k_o is the constant of the equation (g /mg.min), E is the energy of activation (J/mol), R is the gas constant (8.314 J/mol K) and T is the temperature (K). Fig. 6 shows that the rate constants vary with temperature according to Eq. (18). The activation energy (16.52 kJ/mol) is calculated from slope of the fitted equation. The K_c and ΔG^0 (free energy change) values are calculated and presented in Table 4. From the table, it is found that the negative value of ΔG^0 indicates the spontaneous nature of adsorption.

Table 4
Thermodynamic parameters for the adsorption of phosphate

Temperature (K)	K_c	ΔG^o (kJ/mol)	ΔH^o (kJ/mol)	ΔS^o (J/mol K)
305	1.089	–2.16	15.162	50.295
313	1.233	–5.45	15.162	50.295
323	1.500	–10.90	15.162	50.295
333	1.805	–16.36	15.162	50.295

Other thermodynamic parameters such as entropy change (ΔS^0) and enthalpy change (ΔH^0) were determined using the van't Hoff equation

$$\log K_c = \frac{\Delta S^0}{2.303R} - \frac{\Delta H^0}{2.303RT} \tag{19}$$

The enthalpy change (ΔH^0) and entropy change (ΔS^0) were obtained from the slope and intercept of the van't Hoff linear plots of ln K_c vs. $1/T$ (Fig. 7). A positive value of enthalpy change (ΔH^0) indicates that the adsorption process is endothermic in nature and the negative value of change in free energy (ΔG^0) show the spontaneous adsorption of phosphate on the adsorbent. Positive values of entropy change show the increased randomness of the solution interface during the adsorption of phosphate on the adsorbent (Table 4). Enhancement of the adsorption capacity of the electrocoagulant (zinc hydroxide) at higher temperatures may be attributed to the enlargement of the pore size and or activation of the adsorbent surface. Using the Lagergren rate equation, first- order rate constants and correlation coefficients were calculated for different temperatures (305–333 K). The calculated

Fig. 6. Dependence of log k_2 with $1/T$ obtained for solution containing initial phosphate concentration equal to 20 mg-P.L^{-1} at pH 7.0 and using current density of 0.05 A.dm^{-2}.
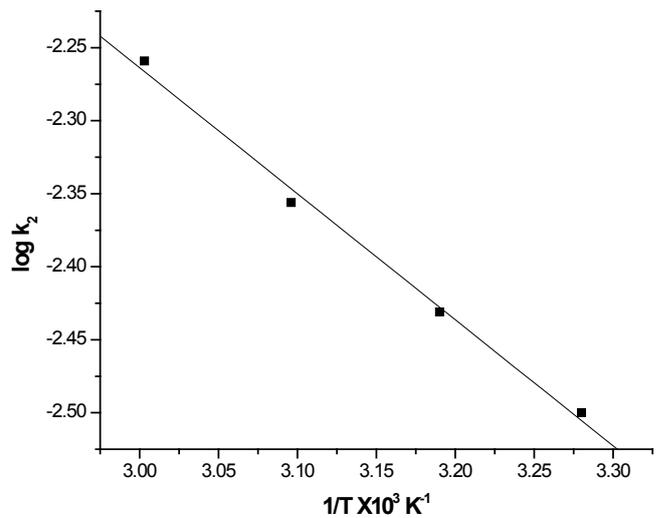
Fig. 7. Dependence of ln K_c wiht $1/T$ obtained for solution containing initial phosphate concentration equal to 20 mg-P.L^{-1} at pH 7.0 and using current density of 0.05 A.dm^{-2}.

q_e values obtained from the first-order kinetics do not agree with the experimental q_e values. The second-order kinetics model shows that the calculated q_e values agree with the experimental values (Table 5). This indicates that the adsorption follows the second-order kinetic model at different temperatures used in this study. From the table, it is found that the rate constant k_2 increased with increasing the temperature from 305 to 333 K. The smaller the k_2 value, the faster the adsorption rate [39]. In present studies the rate constant k_2 value is very low, so the phosphate adsorption rate is fast. The increase in adsorption may be due to a change in pore size upon increasing in kinetic energy of the phosphate species and the enhanced rate of intraparticle diffusion of the adsorbate.

SEM images of zinc electrode, before and after, electrocoagulation of phosphate electrolyte was obtained to compare the surface texture. Fig. 8a shows the original zinc plate surface prior to its use in electrocoagulation experiments. The surface of the electrode is uniform except for a few dents on the surface. Fig. 8b shows the SEM of the same electrode after several cycles of use in electrocoagulation experiments. The electrode surface is now found to be rough, with a number of dents of ca. 1.0 mm. These dents are formed around the nucleus of the active sites where the electrode dissolution results in the production of zinc hydroxides. The formation of a large number of dents may be attributed to the anode material consumption at active sites due to the generation of oxygen at its surface. Electrocoagulation by-product showed the well crystalline phase such as zinc phosphate hydrates and small amount of zinc hydroxide (Fig. 9).

4. Conclusions

The results showed that the maximum removal efficiency of 98.8% was achieved at a current density of 0.05 A.dm^{-2} and a pH of 7 using zinc as the anode and stainless steel as the cathode. The zinc hydroxide generated in the cell remove the phosphate present in the water and reduced the phosphate concentration to 1.2 mg-P.L^{-1}, making it drinkable. The results indicate that the process
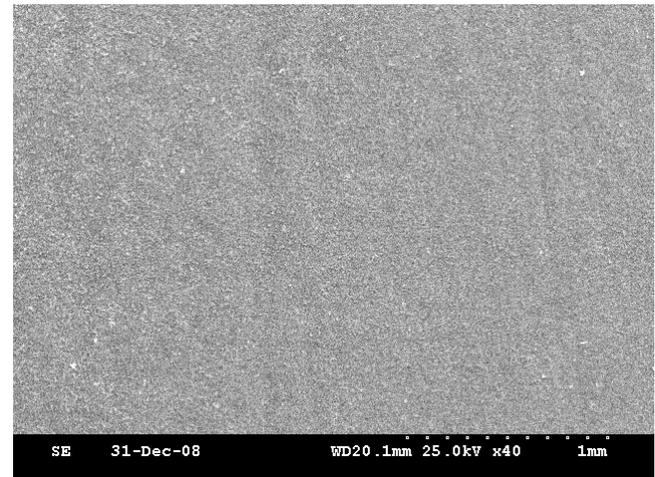
(a)
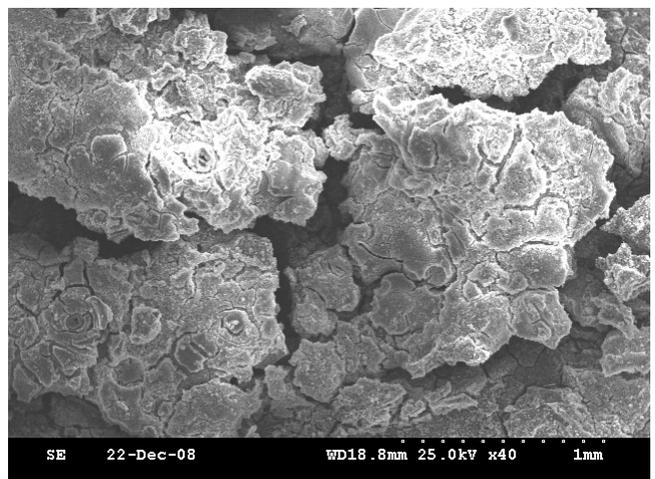
(b)

Fig. 8. SEM images of zinc anode (a) before and (b) after electrocoagulation of phosphate electrolyte.

Fig. 9. XRD diffractogram showing electrocoagulation by-product of the zinc anode.

Table 5
Comparison between the experimental and calculated qe values for different temperature in second order adsorption isotherm at initial concentration 20 mg-P.L^{-1}

Temperature (K)	q_e experimental (mg/g)	k_2 (g/mg min)	q_e calculated (mg/g)	R^2
305	78.28	0.0032	78.27	0.999
313	78.40	0.0037	79.12	0.999
323	78.43	0.0044	78.25	0.999
333	79.63	0.0054	79.04	0.999

can be scaled up to higher capacity and used to eradicate an eutrophication problem. The adsorption of phosphate preferably fitting the Langmuir adsorption isotherm suggests monolayer coverage of adsorbed molecules. The adsorption process follows second-order kinetics. Temperature studies showed that adsorption was endothermic and spontaneous in nature.

Acknowledgments

References

[1] E. Oguzi, A. Gurses and M. Yalcin, Water Air Soil Pollut., 148 (2003) 279–287.
[2] Central Pollution Control Board, Ministry of Environment and Forests, Govt. of India, Delhi, http://www.cpcb.nic.in.
[3] O. Groteruda and L. Smoczynski, Water Res., 20 (1986) 667–669.
[4] S. Yeoman, T. Stephenson, J.N. Lester and R. Perry, Environ. Pollut., 49(3) (1988) 183–233.
[5] J.P. Boisvert, T.C. To, A. Berrak and C. Jolicoeur, Water Res., 31(8) (1997) 1939–1946.
[6] K. Fytianos, E. Voudrias and N. Raikos, Environ. Pollut., 101(1) (1998) 123–130.
[7] R.D. Neufeld and G. Thodos, Environ. Sci. Technol., 3 (1969) 661–667.
[8] H.D. Stensel, Principles of Biological Phosphorus Removal: Phosphorus and Nitrogen Removal from Municipal Wastewater — Principles and Practice, 2nd ed., H.K. Lewis, London, 1991.
[9] Y.Z. Li, C.J. Liu, Z.K Luan, X.J. Peng, C.L. Zhu, Z.Y. Chen, Z.J. Zhang, J.H. Fa and Z.P. Jia, J. Hazard. Mater., 137B(1) (2006) 374–383.
[10] L. Johansson and J.P. Gustafsson, Water Res., 34(1) (2000) 259–265.
[11] B. Kostura, H. Kulveitova and J. Lesko, Water Res., 39(9) (2005) 1795–1802.
[12] E. Oguz, J. Hazard. Mater., 114B (2004) 131–137.
[13] S. Karaca, A.Gurses, M. Ejer and M. Acikyildiz, J. Hazard. Mater., 128B (2006) 273–279.
[14] Y. Yang, D. Tomlinson, S. Kennedy and Y.Q. Zhao, Water Sci. Technol., 54 (2006) 207–213.
[15] S.H. Lee, B.C. Lee, K.W. Lee, S.H. Lee, Y.S. Choi and K.Y. Park, Water Sci. Technol., 55 (2007) 169–176.
[16] D.W. Miwa, G.R.P. Malpass, S.A.S. Machado and A. Motheo, Water Res., 40(17) (2006) 3281–3289.
[17] E. Onder, A.S. Koparal and U.B. Ogutveren, Separ. Purif. Technol., 52 (2007) 527–532.
[18] M. Ikematsu, K. Kaneda, M. Iseki and M. Yasuda, Sci. Total Environ., 382(1) (2007) 159–164.
[19] N. Drouiche, H. Lounici, M. Drouiche, N. Mameri and N. Ghaffour, Desal. Wat. Treat., 7 (2009) 236–241.
[20] P.A. Christensen, T.A. Egerton, W.F. Lin, P. Meynet, Z.G. Shaoa and N.G. Wright, Chem. Commun., 38 (2006) 4022–4023.
[21] K.V. Radha, V. Sridevi, K. Kalaivani and M. Raj, Desal. Wat. Treat., 7 (2009) 6–11.
[22] C. Gabrielli, G. Maurin, H Francy-Chausson, P. Thery, T.T.M. Tran and M. Tlili, Desalination, 201 (2006) 150–163.
[23] X. Chen, G. Chen and P.L. Yue, Chem. Eng. Sci., 57 (2002) 2449–2455.
[24] G. Chen, Separ. Purif. Technol., 38(1) (2004) 11–41.
[25] N. Adhoum and L. Monser, Chem. Eng. Process., 43 (2004) 1281–1287.
[26] R.K. Rajeshwar and J.K. Ibanez, Environmental Electrochemistry, Academic Press, San Diego, 1997.
[27] APHA, Standard Methods for Examination of Water and Wastewater. American Public Health Association, Washington, 1998.
[28] C. Namasivayam and K. Prathap, J. Hazard. Mater., 123B (2005) 127–134.
[29] J. Vanmuylder and M. Pourbaix, In Atlas of Electrochemical Equilibria in Aqueous Solutions: Zinc, J. Vanmuylder and M. Pourbaix, eds., Pergamon, New York, 1966, p. 409.
[30] A.K. Golder, A.N. Samantha and S. Ray, Separ. Purif. Technol., 52(1) (2006) 102–109.
[31] S. Irdemez, N. Demircioglu, Y.S. Yildiz and Z. Bingul, Separ. Purif. Technol., 52(2) (2006) 218–223.
[32] O. Groterud and L. Smoczynski, Water Res., 20(5) (1986) 667–669.
[33] Lagergren, Euro. Poly. J., 24(4) (1898) 1–39.
[34] G. McKay and Y.S. Ho, Water Res., 33(2) (1999) 578–584.
[35] C. Namasivayam and S. Senthil Kumar, Ind. Eng. Chem. Res., 37(12) (1998) 4816–4822.
[36] F.H. Uber, Z. Phys. Chem., 57 (1985) 387–470.
[37] I. Langmuir, J. Am. Chem. Soc., 40 (1918) 1361–1365.
[38] L.D. Michelson, P.G. Gideon, E.G. Pace and L.H. Kutal, US Department of Industry, Office of Water Research and Technology Bulletin, 1975.
[39] W. Nigussie, F. Zewgeb and B.S. Chandravanshi, J. Hazard. Mater., 147(3) (2007) 954–963.
[40] S. Nayak Preeti and B.K. Singh, Res. J. Chem. Environ., 11 (2007) 23–28.
[41] X.-Y. Yang and B. Al-Duri, Chem. Eng. J., 83(1) (2001) 15.
[42] P.Y. Hering Chen, J.A. Wilkie and M. Elimelech, J. AWWA, 88 (1996) 155–167.